Slow inactivation and reactivation of the K^+ channel in squid axons

A tail current analysis

John R. Clay

Laboratory of Biophysics, Division of Intramural Research, National Institute of Neurological, Communicative Disorders, and Stroke, National Institutes of Health, Bethesda, Maryland 20892; and Marine Biological Laboratory, Woods Hole, Massachusetts 02543

ABSTRACT Potassium current inactivation and reactivation in squid axons were measured from tail current amplitudes after voltage clamp prepulses to the potassium equilibrium potential, E_K, in seawater containing elevated levels of potassium ion concentration, K_o. Little or no inactivation resulted with prepulses lasting < 100 ms. Longer pulses caused the current to inactivate in two phases, one between 0.1 and 1 s, and a second phase between 5 and 100 s. Inactivation was incomplete. The time constant of the tail current after a prepulse to E_K was independent of pulse duration (0.1–120 s). Inactivation was independent of K_o ($10 \leq K_o \leq 300$ mM), and it was independent of membrane potential, V, for $-40 \leq V \leq 0$ mV. Reactivation was measured with a three-pulse protocol. The reactivation time course was sigmoidal with a delay of ~100 ms before significant reactivation occurred. These results were described by a model consisting of three inactivated states arranged in a linear sequence. The rate constants of the model are of the form $(A + B \exp(CV))$, or $1/(A + B \exp(CV))$, which are required to describe the noninactivating conductance component.

INTRODUCTION

The delayed rectifier potassium channel in squid axons inactivates during sustained depolarizing voltage clamp pulses. This effect was originally reported by Ehrenstein and Gilbert (1966), who found that inactivation occurred with a single, voltage-dependent time constant in the 10–30-s range. Surprisingly, no additional results were reported on this effect in squid axons until the work of Chabala (1984), who found that the inactivation kinetics were second order. Both reports lack information concerning the onset of inactivation and reactivation during the initial 1–2 s of each process. I have filled in these gaps using a technique similar to that of Ehrenstein and Gilbert (1966). These results demonstrate that inactivation and reactivation both occur after a delay of ~100 ms. The delay in reactivation is particularly significant, because it can be used to distinguish between models of the inactivation process. In particular, these results are suggestive of a model consisting of multiple inactivated states, rather than a model consisting of multiple open states proposed by Chabala (1984).

METHODS

Experiments were performed on voltage-clamped, internally perfused squid giant axons using methods that have been previously described (Clay and Shlesinger, 1983). The temperature ranged between 7 and 10°C. It was maintained constant to within ±0.1°C during any single experiment. The internal perfusate consisted of 250 mM K glutamate, 25 mM K_2HPO_4, and 370 mM sucrose. The external artificial seawater (ASW) contained either 10, 50, 100, 150, or 300 mM KCl with, respectively, 430, 390, 340, 290, or 140 mM NaCl. The ASW also contained 50 mM $MgCl_2$, 10 mM $CaCl_2$, 10 mM Tris-HCl, and 0.5 μM tetrodotoxin. Liquid junction potentials were <3 mV. The results in this study have not been corrected for these relatively small voltage offsets. The tail current amplitudes in the experiments with $K_o \geq 100$ mM were measured 100 μs after return of the membrane potential to the holding level.

Address correspondence to John R. Clay, Laboratory of Biophysics, National Institutes of Health, Building 9, Room 1E127, Bethesda, MD 20892.

RESULTS

The basic inactivation effect with normal ionic conditions (K_o = 10 mM) is illustrated in Fig. 1. In this experiment the membrane potential was held either at −90 or −60 mV for several minutes before a step to +50 mV. The step to +50 from −90 mV elicited a significantly greater outward current than the step from −60 mV. Approximately 30% of the conductance was inactivated in steady state at −60 mV. Appreciably more inactivation occurred at −50 mV. The kinetics of this effect were measured as described in Fig. 2. In this experiment the potential was stepped from a holding level of −90 to −50 mV for various different times between 0.1 and 350 s, followed by a step to 0 mV. The maximum outward current elicited by the step to 0 mV is plotted in Fig. 2 as a function of the duration of the step to −50 mV. These results are consistent with a second order inactivation process. The time constants of inactivation were, approximately, 0.3 and 30 s. The onset of inactivation cannot be clearly

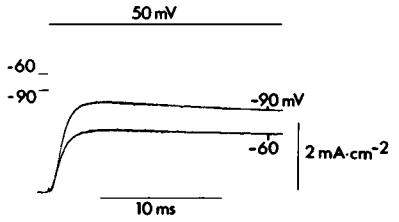

FIGURE 1 Steady-state inactivation of I_K at −60 mV. Membrane potential was held either at −90 or −60 mV for 3 min. The potential was then stepped to +50 mV. K_o = 10 mM.

determined with this protocol because of ion accumulation. That is, potassium ions accumulate with outward current in the space between the axonal membrane and the Schwann cell surrounding the axon, thereby reducing the current during a single pulse. This mechanism is responsible for the slight decline in the records in Fig. 1 (Clay, 1984, 1986). However, these results alone cannot distinguish between inactivation and ion accumulation. Moreover, inactivation for potentials positive to −50 mV cannot be readily measured with the protocol in Fig. 2, because a significant fraction of the conductance is activated by prepulses positive to −50 mV. An alternative method is required for these results.

The procedure I have used is to elevate the external potassium ion concentration so that E_K, the equilibrium potential, lies within the range of activation of the conductance. The activation kinetics are not altered by this procedure (Clay, 1984; Armstrong and Matteson, 1986). A prepulse to E_K under these conditions will activate the conductance without producing significant, net current flow. An inward current will flow through the activated conductance immediately after return of the membrane potential to the holding level, which deactivates with a time constant appropriate to the holding potential. An example of results obtained with this protocol are shown

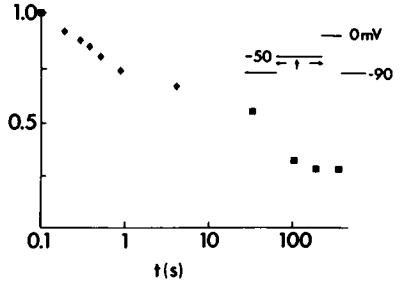

FIGURE 2 Kinetics of inactivation at −50 mV. The membrane potential was held at −90 mV for 3 min followed by a step of variable duration, t, to −50 mV, and then a 20 ms duration step to 0 mV. The maximum outward current elicited by the step to 0 mV is shown as a function of t. K_o = 10 (♦) or 50 mM (■).

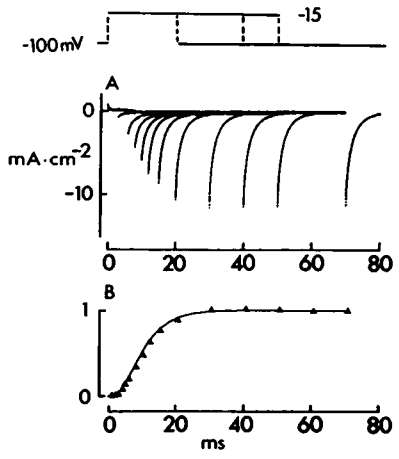

FIGURE 3 I_K activation kinetics as determined from tail current amplitudes. The inset at the top illustrates the basic protocol. The external potassium ion concentration was elevated so that E_K was within the activation range of the conductance. In this case K_o = 150 mM and E_K = −15 mV. The membrane potential was stepped to −15 mV and then back to the holding level, −100 mV. (*A*) Superimposed records of tail currents after a prepulse to −15 mV of duration indicated on the abscissa. (*B*) Amplitude of the tail currents in *A* normalized by the amplitude of the 30-ms prepulse result. The solid line is a best fit, by eye, to these results of $(1 - \exp(-t/\tau))$, with τ = 5.5 ms.

in Fig. 3 *A* for an axon with 150 K_o (prepulse potential of −15 mV) for various different prepulse durations. The relative tail current amplitudes are shown in Fig. 3 *B* along with the best fit (by eye) to these results of the Hodgkin and Huxley (1952) model of K^+ conductance, $(1 - \exp(-t/\tau))^4$, with τ = 5.5 ms. These and other results (Clay, 1984) show almost no inactivation for pulse durations up to 100 ms. At most, the conductance (tail current amplitude) declined by 3% (10 axons).

The logical continuation of the experiment in Fig. 3 *A* with significantly longer prepulse durations is illustrated in Fig. 4 for an axon in 100 K_o and a prepulse potential of −25 mV. The prepulse duration is indicated on the abscissa in Fig. 4. A 15-s rest interval between each prepulse was used to allow full reactivation to occur (see below). The tail currents show a clear reduction in amplitude (inactivation at −25 mV) from 0.1 to 1.0 s, and a second phase of inactivation from 4 to 100 s. (Note the change of time scale in Fig. 4 at the 4 s mark). The inset at the bottom right of Fig. 4 illustrates the tail current with a 0.3-s prepulse before (record *a*) and after (record *b*) the results in Fig. 4 were obtained. These results are approximately the same, which indicates a lack of significant rundown of the conductance during the experiment.

The relative tail current amplitudes with 100 K_o and a prepulse of −25 mV from four different axons as a function of time on a logarithmic time scale are shown in

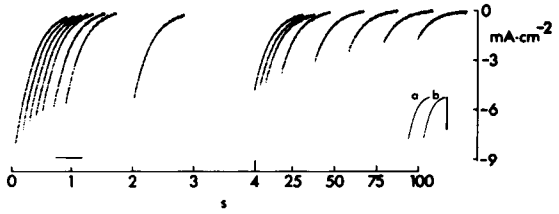

FIGURE 4 Tail currents for a prepulse to −25 mV (K_o = 100 mM) of duration indicated on the abscissa. Note change of scale at 4 s. The horizontal bar above the 1 s time mark indicates 10 ms, which is the scale for each record shown. The inset at the lower right shows the tail current for a 0.3-s prepulse before (*a*) and after (*b*) this experiment. The vertical bar alongside record *b* indicates 5 mA · cm^{-2}.

Fig. 5 along with the activation kinetics from Fig. 3 *A*. These results in 100 K_o are similar to the results obtained in 10 and 50 K_o in Fig. 2. The solid line in Fig. 5 is a best fit (by eye) to these data of the model described below. The inset in the upper right corner of Fig. 5 illustrates the tail currents with a prepulse of 0.1, 120, 140, and 0.1 s again, labeled *a*, *b*, *c*, and *d*, respectively. These results, and similar results with 400-s prepulse durations (Fig. 5), show that the inactivation process reaches a steady state at ~120 s leaving a relative, noninactivating conductance of ~20%.

The tail currents for prepulse durations of 0.1, 0.7, 5, and 80 s from the experiment in Fig. 5 are shown on a semilogarithmic scale in Fig. 6. These records are well described by a single exponential function of time with a time constant which is not appreciably altered by the prepulse duration (Fig. 6 legend).

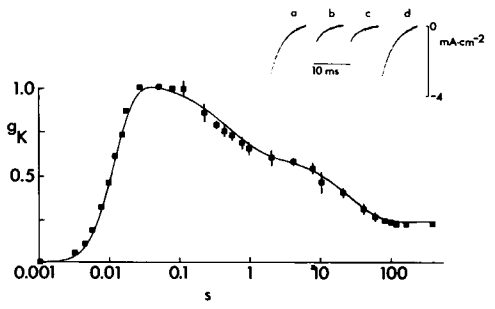

FIGURE 5 Potassium channel activation and inactivation kinetics on a logarithmic time scale. The symbols for times <0.1 s were taken from Fig. 3*B*. The results for times ≥0.1 s are the average ±SD from four axons with a prepulse to −25 mV (K_o = 100 mM). Holding potential = −100 mV. All results were normalized to the 20 ms data point. The solid line is a description of these data by $n^4(t)p(t)$, where $n(t) = (1 - \exp(-t/\tau))$ with τ = 5.5 ms, and $p(t)$ is the probability that the conductance is not inactivated, based on the three inactivated state model given in the text. Inset at the upper right shows records from an axon with a prepulse duration of 0.1, 120, 140, and 0.1 s, labeled *a*, *b*, *c*, and *d*, respectively.

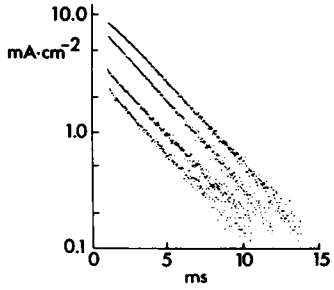

FIGURE 6 Semilogarithmic plot of the tail currents in Fig. 3 for, top to bottom, 0.1, 0.7, 5, and 80 s. The best single exponential fits to these records had time constants of 3.24, 2.97, 3.47, and 3.17 ms, respectively.

The effect of membrane potential on inactivation kinetics was tested with 150 K_o and prepulse potentials of −30, −20, and −10 mV (Fig. 7). The tail current amplitudes increased with the depolarizing level (Fig. 7 *A*), although the kinetics of inactivation were not affected, as shown in Fig. 7 *B*, which contains the results in Fig. 7 *A*, scaled so as to produce maximum overlap, by eye, of the data points from the three different potentials. No discernible effect of membrane potential was apparent.

The effect of K_o on inactivation was tested with a prepulse to −10 mV with K_o = 100 and 300 mM. This change in K_o has been shown to alter the tail current time course (Swenson and Armstrong, 1981; Matteson and

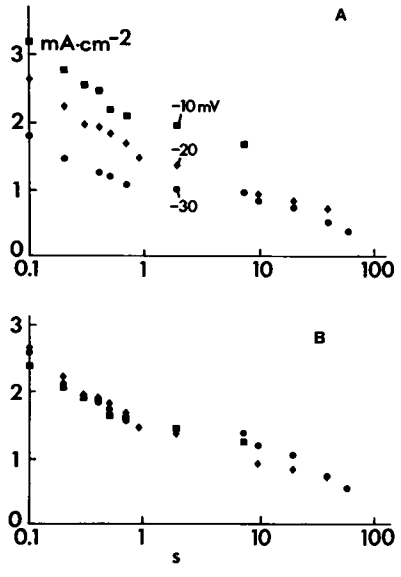

FIGURE 7 Lack of effect of membrane potential on inactivation in the −30 to −10 mV range. (*A*) Tail current amplitudes with 150 mM K_o and prepulses to −10 (■), −20 (♦), and −30 mV (●). Holding potential was −100 mV. (*B*) Same results as in *A* with the −10, −20, and −30 mV results scaled by 0.8, 1.0, and 1.45, respectively.

Swenson, 1986; Clay, 1986), although the activation rate is unaffected (Clay, 1984; Armstrong and Matteson, 1986). I have found that the effect of K_o on tail current kinetics does not always occur, and that it is independent of voltage in axons in which it does occur, which suggests that the effect is not related to the permeation pathway (Clay, 1986; 1988). Consequently, there is no reason, *a priori,* to expect that K_o would alter inactivation kinetics. The results in Fig. 8 demonstrate that an increase of K_o from 100 to 300 mM does not alter inactivation kinetics, even in preparations in which tail kinetics are affected. The records in the top panel in Fig. 8 demonstrate inactivation for prepulse durations in the 0.1–0.7–s range with 100 and 300 K_o. Approximately the same degree of inactivation occurred with both potassium levels even though the tail current time constant was increased by a factor of 1.7. The results in the bottom panel of Fig. 8 from another preparation in which the tail current time constant was also increased further show a lack of effect of K_o on inactivation. These results were scaled so that they overlapped, by eye, as much as possible.

The similarity of inactivation results throughout this study with $10 \leq K_o \leq 300$ mM suggests that inactivation is independent of K_o. A similar observation was reported by Ehrenstein and Gilbert (1966) in their original work.

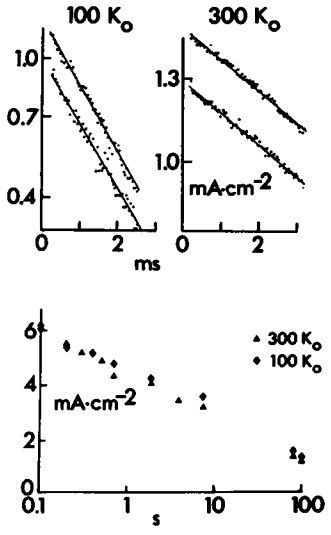

FIGURE 8 Lack of effect of external potassium on inactivation. The top panels show tail currents on a semilogarithmic scale for prepulses to −10 mV of duration 0.1 and 0.7 s (*left*) and 0.1 and 0.5 s (*right*) showing reduction of tail current amplitude (inactivation). The lines are the best single exponential fits to these records with time constants of 2.32 (*top*) and 2.40 ms (*bottom*) for the top left panel, and 4.45 (*top*) and 4.35 ms (*bottom*) for the right hand panel. Shown below are similar results from another preparation with the 100 and 300 K_o results scaled so that they overlap as much as possible.

Moreover, inactivation is independent of membrane potential for $-40 \leq V \leq 0$ mV. Inactivation is incomplete and it occurs in two kinetic phases. Similar results were observed in all experiments ($n = 24$).

The protocol used to measure reactivation is illustrated in Fig. 9. The membrane potential was held at E_K (0 mV in Fig. 9 with $K_o = 300$ mM) for 3 min to allow inactivation to reach steady state. It was then stepped to a hyperpolarized level (−100 mV) which elicited the tail current of the noninactivating component. The potential was held at the hyperpolarized level for a variable period of time to allow reactivation to occur. It was then stepped back to E_K for 20 ms to activate the conductance without significant net current flow. The potential was then stepped again to the hyperpolarized level to elicit the tail current. Finally, the potential was returned to E_K for 3 min before repeating the three-step sequence. This protocol is illustrated in Fig. 9 for durations of the initial step to −100 mV of 40 and 60 ms. The tail currents elicited by the second step to −100 mV from another preparation with $K_o = 100$ mM ($E_K = -25$ mV) are shown in Fig. 10 as a function of the duration of the first step to −100 mV. These results describe a sigmoidal time dependence of reactivation, and they show that reactivation is complete (at −100 mV) within 4 s. One possible explanation for the sigmoidal kinetics could be that the 20-ms pulse to E_K is inactivating the reactivated component, thereby complicating interpretation of the reactivation kinetics. This effect appears to be unlikely, based on the results in Fig. 3, which show essentially no inactivation for pulse durations at E_K of up to 100 ms. Nevertheless, I tested this point directly by measuring reactivation kinetics with both a 20- and a 40-ms prepulse. These results (not

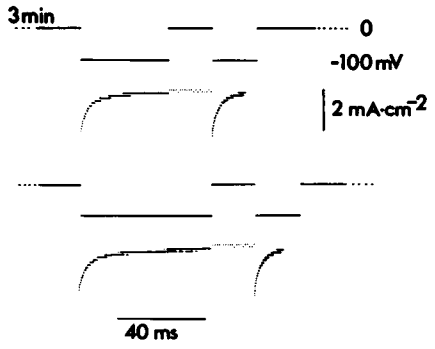

FIGURE 9 Protocol for measuring reactivation kinetics. The membrane potential was held at E_K (0 mV in this case with 300 K_o) for 3 min to allow inactivation to reach steady state. The potential was then stepped to −100 mV for 40 ms in the top panel and 60 ms in the bottom panel. The tail current of the noninactivating component was elicited by this first step. The potential was then stepped back to E_K for 20 ms, followed by a second step to −100 mV.

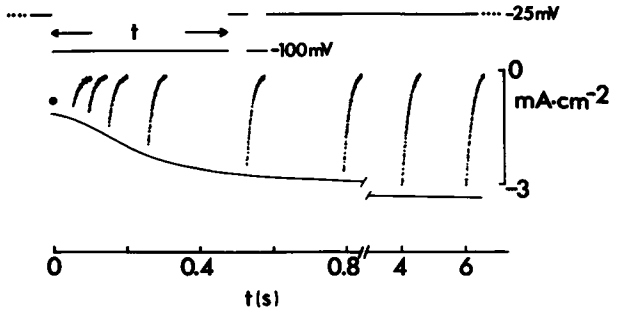

FIGURE 10 Tail currents as a function of the duration of the first step to −100 mV in the protocol illustrated in Fig. 9 for an axon in 100 mM K_o with a prepulse to −25 mV. The voltage steps above the records illustrate the protocol for the 525 ms record. The symbol (●) represents the amplitude of the tail current elicited by the first step to −100 mV. The line below the records was drawn by eye to illustrate the sigmoidal time dependence of these results.

shown) indicate that the delay in reactivation is independent of pulse duration. This kinetic feature was observed in all measurements of reactivation (n = 7).

Reactivation kinetics as a function of potential are shown in another preparation (Fig. 11) for −55, −65, −75, and −85 mV, along with a theoretical description from the model given below (Discussion). The experimental results at each potential were scaled by the amplitude of the steady-state level of the reactivated tail current. The latter result was compared with the steady-state, reactivated tail current at −100 mV, which was assumed to represent full reactivation of the conductance. Appropriate corrections for the changes in driving force were made at each potential in this analysis. These results demonstrate that full reactivation occurred at −75 and −85 mV, but not at −55 and −65 mV. The relative steady-state reactivation and inactivation results from five different preparations are shown in Fig. 12 along with a theoretical description from the model given below. Also shown in Fig. 12 are results from experiments in 10 mM K_o (◇) in which inactivation was measured at −60 and −50 mV from a holding potential of −90 mV, as described in Fig. 1.

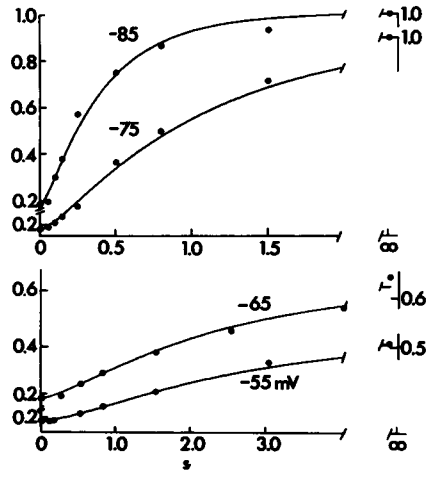

FIGURE 11 Voltage dependence of reactivation kinetics. These results were obtained from a holding potential of −25 mV (K_o = 100 mM) with hyperpolarizing pulses in the protocol of Fig. 9 to the potentials indicated. The curves were derived from the three state inactivation model described in the text with a = 0.36, 0.3, 0, 0; b = 1.05, 1.5, 4.0, 12; c = 1.6, 2, 5, 10; d = 4.8, 6, 7, 15; e = 3.25, 4, 15, 30; and f = 0.8, 1, 9, 18 s^{-1} for, respectively, −55, −65, −75, and −85 mV.

DISCUSSION

The experimental results given above, in particular the reactivation kinetics, suggest that the slow kinetics of the potassium conductance can be described by a linear sequence of some number of inactivated states. A reasonable fit to the data was found with three inactivated states, which appears to be the minimum number required. The model is given by

$$NI \underset{b}{\overset{a}{\rightleftharpoons}} I_1 \underset{d}{\overset{c}{\rightleftharpoons}} I_2 \underset{f}{\overset{e}{\rightleftharpoons}} I_3,$$

where NI refers to the noninactivated state of the channel, which could be either the open state, or any one of the closed states. The channel does not necessarily have to open before inactivating. It could go, with equal probability, from any closed state to the inactivated state, I_1. The results in this study cannot distinguish between these two possibilities, essentially because the activation kinetics are so much more rapid than the inactivation kinetics. I have assumed that inactivation is independent of activa-

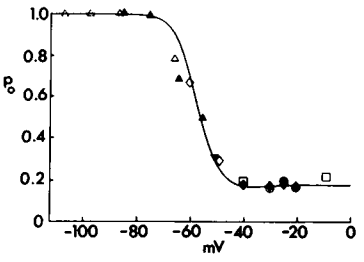

FIGURE 12 Steady-state inactivation, as determined from inactivation and reactivation experiments. Each symbol represents a different axon. The curve represents p_o as given in Eq. 1 with a = {1 + exp [−(V + 55)/5]}$^{-1}$, b = 1.75 + exp [−(V + 70)/10]; c = 1 + exp [−(V + 62)/10]; d = 2 + exp [−(V + 55)/15]; e = 0.2 + exp [−(V + 40)/8]; and f = 0.015 + exp [−(V + 45)/5] s^{-1}.

tion, so that the probability that the channel is open is given by $n^4(t)p(t)$, where $n^4(t)$ represents the relative activation kinetics, with $n(t) = (1 - \exp(t/\tau))$, and τ = 5.5 ms for the results in Fig. 3, and $p(t)$ is the probability that the channel is not inactivated. The latter quantity can be determined analytically from the model. In particular, the probability p_o that the channel is not inactivated in the steady state is given by

$$p_o = [1 + a/b + (ac)/(bd) + (ace)/(bdf)]^{-1}. \quad (1)$$

The solid line in Fig. 12 was calculated from Eq. 1 with the empirically derived equations for the rate constants given in the legend of Fig. 12. The kinetics of the model were determined from numerical iteration. This procedure was used to fit the results in Fig. 5. The rate constants $a, b, \ldots f$ were chosen by trial and error so as to produce the best fit, by eye, to the data. The result of this analysis is shown by the solid line in Fig. 5 with $a = c = 1$ s^{-1}, $b = d = 2$ s^{-1}, and $e = 0.2$ s^{-1} and $f = 0.015^{-1}$ s. The model provides a good overall description to the data in Fig. 5, although it predicts 7% inactivation at 100 ms, whereas no more than 3% inactivation was ever observed for pulses of this duration. A comparable fit to these results could also be obtained with only two inactivated states. The third state, I_3, was required to produce a reasonable fit to the reactivation kinetics. This analysis is illustrated in Fig. 11. (The various rate constants of the fits are given in the legend of Fig. 11.) The model provides a good overall description of these results, although it fails to completely describe the sigmoidal time dependence of the data.

The above analysis is to be contrasted with that of Chabala (1984), who assumed that the rate constants were necessarily of the form $\exp(AV + B)$. This assumption explicitly excludes the model given above, because it predicts $p_o = 0$ at depolarized potentials with rate constants of the form $\exp(AV + B)$ whereas $p_o > 0$, that is, a noninactivating component, is observed in this potential range. Rate constants of the form $[A + B \exp(CV)]^{\pm 1}$ are required in this model to give $p_o > 0$ as $V \rightarrow \infty$. That is, $a, b, \ldots f$ must all be finite at depolarized potentials. Chabala (1984) concluded that the only model based on a homogeneous population of channels which could explain this result was one in which the channel had multiple open states with a different conductance for each state. However, his model does not predict sigmoidal reactivation, as illustrated in Fig. 13. The data points in Fig. 13 were taken from Fig. 10. Curve *a* in Fig. 13 is a description of these results by the Chabala (1984) model, which has three open states and no inactivating states. Curve *b* is taken from the model given above, which contains three inactivated states. As noted, this model underestimates the degree of sigmoidicity in the data. However, it is at least qualitatively consistent with the data. The Chabala (1984) model predicts no sigmoidicity.

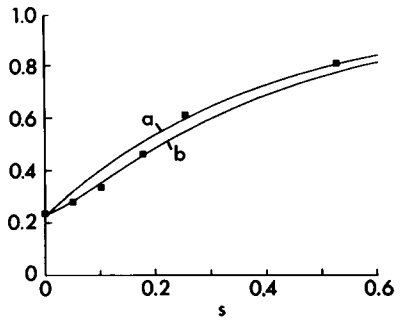

FIGURE 13 Comparison of the Chabala (1984) model of inactivation and the model given in the text with the reactivation kinetics from Fig. 10 (■). Curve *a* is the prediction of the three open state model of Chabala (1984), his model 5, with $a_{01} = \exp(0.091\ V + 2.61)$; $a_{12} = \exp.(0.002\ V + 2.35)$; $a_{10} = \exp(-0.044\ V - 4.81)$; and $a_{21} = \exp(-0.103\ V - 8.25)\ s^{-1}$ ($V = -100$ mV) with relative conductances of the three states given by 1, 0.73, and 0.23 for state 0, 1, and 2, respectively. Curve *b* is the prediction of the three inactivated state model with $a = b = 1\ s^{-1}$; $c = d = 2\ s^{-1}$; $e = 0.2\ s^{-1}$, and $f = 0.015\ s^{-1}$.

An alternative explanation for the noninactivating component, suggested by Chabala (1984), is that it may be attributable to a second type of channel. The results in this study cannot exclude this model, although the tail current kinetics in Fig. 6 are consistent with a homogeneous channel population. Preparations in which more than a single type of channel have been reported usually show a dependence of the tail current time constant on the duration of a voltage prepulse, especially relatively long lasting prepulses (Dubois, 1981). The results in Fig. 6 do not clearly show this effect. These and other results (Clay, 1984) suggest that a second component, if present, contributes a relatively small amount of the total potassium ion current. Single channel recordings from cut-open axons are not inconsistent with this view (Llano et al., 1988). Moreover, the noninactivating component does not necessarily require a second type of channel. The assumption by Chabala (1984) which leads to this conclusion is based on the analysis of Stevens (1978), who demonstrated that the rate constants are, in general, of the form $\exp(-U(V)/kT)$, where k is the Boltzmann constant, T is the temperature, and U is the free energy difference between two conformational states of the channel. The simplest assumption for $U(V)$ is $U = AV + B$. However, other possibilities cannot be excluded, because essentially nothing is known from first principles about the voltage dependence of this quantity. For example, consider a model with a single inactivated state with the energy profile governing transitions of the gating charge as described in Fig. 14. The energy wells labeled 0 and 1

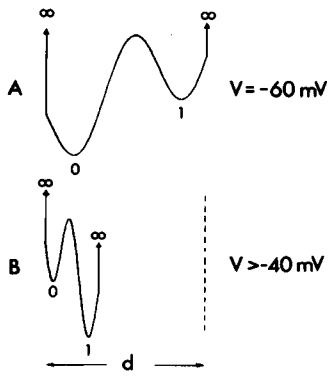

FIGURE 14 Free energy diagrams for the model of inactivation described in the text. (*A*) Free energy profile for $V = -60$ mV. The energy well labeled 0 represents the noninactivated state. The well labeled 1 represents the inactivated state. The energy barrier between the two states is approximately at the midpoint of the electrical field of the membrane. The locations of the states are assumed to be independent of membrane potential for $V < -60$ mV. The arrows pointing to infinity on either side of the membrane represent barriers which constrain the inactivation gating charge to the membrane. (*B*) Free energy profile for $V > -40$ mV. Under these conditions, the locations of the states are assumed to be changed so that they are very close to the inner edge of the membrane. The right hand constraining barrier has also been shifted.

represent the noninactivating and inactivated states, respectively. The positions of these wells are assumed to be independent of membrane potential for $V < -60$ mV. The arrows pointing toward ∞ on either side of the profile represent barriers which constrain the gating charge to the membrane. The barrier which separates the two states lies well within the electric field of the membrane. Consequently, the transitions between the states are voltage dependent for $V < -60$ mV. For potentials positive to -60 mV, especially $V > -40$ mV, the energy profile is assumed to be constrained near the inner surface of the membrane. The energy barrier between the two states now lies nearly outside of the electric field of the membrane. Consequently, transitions between the two states will be weakly voltage dependent in this potential range. This hypothetical scheme is one way in which the model I have used might be physically realized.

Incomplete inactivation in two kinetic phases occurs in squid axons, as noted here and by Chabala (1984), in pufferfish supramedullary neurons (Nakajima and Kusano, 1966), frog myelinated nerve (Schwarz and Vogel, 1971), and cultured neuroblastoma cells (Moolenaar and Spector, 1978). A delay in reactivation has not been previously reported. Perhaps the best known example of an inactivating potassium current is the rapidly inactivating I_A component first reported in molluscan neurons by Connor and Stevens (1971). However, the time constant of inactivation of I_A is two or three orders of magnitude less than that of the delayed rectifier, I_K. The slower phase of I_K inactivation in squid is ~30 s, as noted above and by Ehrenstein and Gilbert (1966). The maximum time constant reported by Chabala (1984) is 11 s, which would appear to be at odds with Ehrenstein and Gilbert (1966) and my results. The reason for this difference is not readily apparent.

The author gratefully acknowledges technical assistance throughout the course of this work by Ruthanne Mueller, Richard Waltz, and Clyde Tyndale.

Received for publication 24 March 1988 and in final form 10 October 1988.

REFERENCES

Armstrong, C. M., and D. R. Matteson. 1986. The role of calcium ions in the closing of K channels. *J. Gen. Physiol.* 87:817–832.

Chabala, L. D. 1984. The kinetics of recovery and development of potassium channel inactivation in perfused squid giant axons. *J. Physiol. (Lond.).* 356:193–220.

Clay, J. R. 1984. Potassium channel kinetics in squid axons with elevated levels of external potassium concentration. *Biophys. J.* 45:481–485.

Clay, J. R. 1986. Potassium ion accumulation slows the closing rate of potassium channels in squid axons. *Biophys. J.* 50:197–200.

Clay, J. R. 1988. A new interpretation of the effects of monovalent cations on potassium channel gating in squid axons. *Biophys. J.* 53:262a.

Clay, J. R., and M. F. Shlesinger. 1983. Effects of external cesium and rubidium on outward potassium currents in squid axons. *Biophys. J.* 42:43–53.

Connor, J., and C. F. Stevens. 1971. Inward and delayed outward membrane current in isolated neural somata under voltage clamp. *J. Physiol. (Lond.).* 213:1–19.

Dubois, J. M. 1981. Evidence for the existence of three types of potassium channels in the frog Ranvier node membrane. *J. Physiol. (Lond.).* 318:297–316.

Ehrenstein, G., and D. L. Gilbert. 1966. Slow changes of potassium permeability in the squid giant axon. *Biophys. J.* 6:553–566.

Hodgkin, A. L., and A. F. Huxley. 1952. A quantitative description of membrane current and its application to conduction and excitation in nerve. *J. Physiol. (Lond.).* 117:500–544.

Llano, I., C. K. Webb, and F. Bezanilla. 1988. Potassium conductance of the squid giant axon. Single-channel studies. *J. Gen. Physiol.* 92:179–196.

Matteson, D. R., and R. P. Swenson, Jr., 1986. External monovalent cations that impede the closing of K channels. *J. Gen. Physiol.* 87:795–816.

Moolenaar, W. H., and I. Spector. 1978. Ionic currents in cultured mouse neuroblastoma cells under voltage-clamp conditions. *J. Physiol. (Lond.).* 278:265–286.

Nakajima, S., and K. Kusano. 1966. Behavior of delayed current under voltage clamp in the supramedullary neurons of puffer. *J. Gen. Physiol.* 49:613–628.

Schwarz, J. R., and W. Vogel. 1971. Potassium inactivation in single myelinated nerve fibers of *Xenopus laevis*. *Pfluegers Arch. Eur. J. Physiol.* 330:61–73.

Stevens, C. F. 1978. Interactions between intrinsic membrane protein and electric field: an approach to studying nerve excitability. *Biophys. J.* 22:295–306.

Swenson, R. P., Jr. and C. M. Armstrong. 1981. K^+ channels close more slowly in the presence of external K^+ and Rb^+. *Nature (Lond.).* 291:427–429.